Swift XRT Response Matrix Files

XRT-LUX-CAL-108

Release Version: RMF-LUX-6.0
Release Date: 15 October 2004

Andrew Beardmore[1], Kallol Mukerjee, Tony Abbey, Julian Osborne, Alan Wells
University of Leicester

1 Introduction

This note describes release v6.0 of the Swift XRT response matrices. Response Matrix Files (RMFs) are released for each spectral mode of the XRT (photon counting mode, windowed timing mode and photodiode mode), for a variety of useful event pattern selections. Additionally in this release, non-event recognition responses are available for windowed timing and photodiode mode, which are suitable for use with the quick look TDRSS spectra collected in these modes.

Improvements to the RMFs with respect to the previous version (prerelease v5.0, 25 March 2004, release note XRT-LUX-CAL-108_RMF_v5) are described below (section 4). Comparison of the RMFs with calibration data are shown in section 6 and their limitations are addressed in section 7.

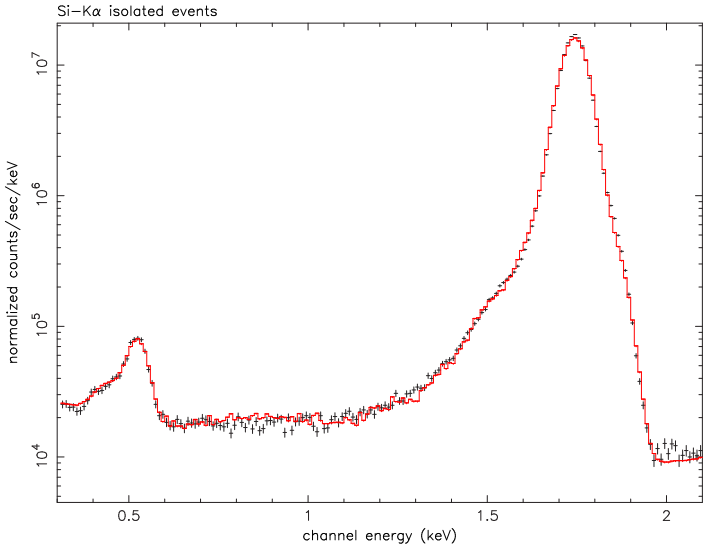

Figure 1: The XRT CCD response model is compared with an isolated event photon counting spectrum as detected by the Leicester facility with a Si-K line source. The histogram (red) shows a model consisting of Si-Kα (1.74 keV), Si-Kβ (1.84 keV), a weak O-Kα (0.525 keV) background line and an underlying bremsstrahlung continuum.

2 Response matrix generation

The RMFs are created by a Monte Carlo simulation code (Mukerjee et al., 2004). The code models the following processes: transmission of the incident X-rays through the CCD electrode structure; photo-absorption in the active layers of the device; charge cloud generation; charge cloud transportation and spreading; silicon fluorescence and associated escape peaks; surface loss effects; mapping the resultant charge cloud to the detector pixel array; charge transfer efficiency; electronic readout noise; event thresholding and classification. Figure 1 shows a fit to laboratory calibration data.

The RMFs are generated using a 5 eV input energy grid, which extends from $0 - 12$ keV, with 10^5 input photons per bin. The resultant spectral response is calculated over 1024 energy channels, the energy scale of which depends on the type of RMF: the event graded RMFs use the PI scale of 10 eV per channel, whereas the non-event recognition RMFs use 10.12 eV per channel (the original PHA scale rebinned by a factor of 4) to match the TDRSS (non-event recognition) spectra.

[1] apb@star.le.ac.uk

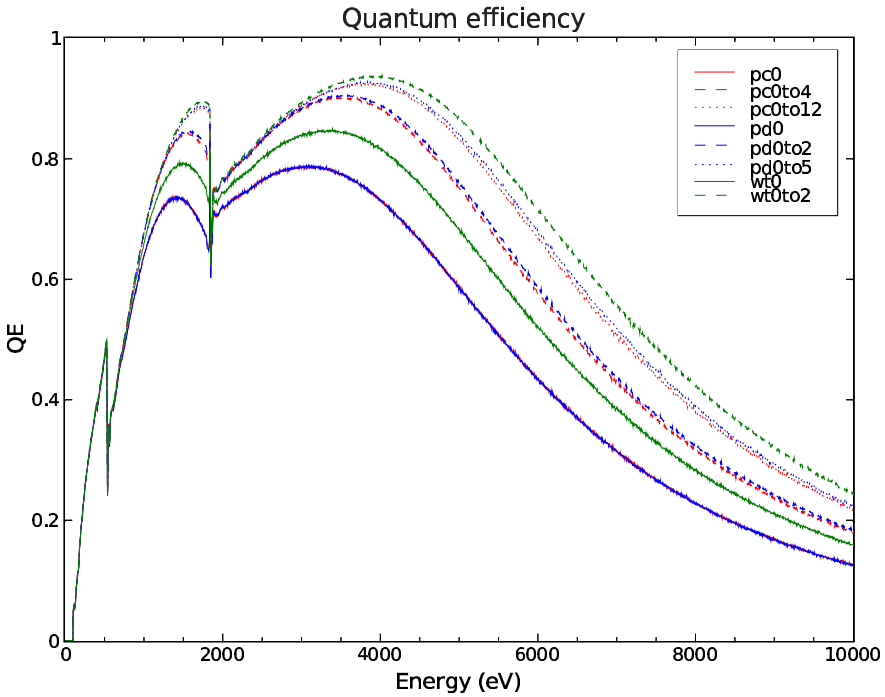

Figure 2: CCD quantum efficiency curves for the various modes and grade selection criteria for the v6 RMF release. Note the grade 0 photon counting and photodiode modes are superimposed.

3 Mode dependant responses

During normal GRB observations the Swift XRT operates autonomously and aquires spectra in three modes depending on the source flux. These are :

(i) Photodiode mode – a fast timing mode, which is achieved by alternating the parallel and serial readouts of the CCD one pixel at a time. As a result no positional information is retained.

(ii) Window timing mode – another fast timing mode which is achieved by reading out the central 200 columns of the CCD and by binning 10 rows at a time. In this mode 1-D positional information is retained.

(iii) Photon counting mode – the traditional 2-D mode of operation for an X-ray CCD detector. In this mode the central pixel of an event, plus the surrounding 3x3 are telemetred.

In photon counting mode X-rays are characterised by events up to 4-pixels in size depending on the energy of the incident X-ray and the corresponding depth of the initial interaction in the detector. Consequently, the quantum efficiency at higher energies is greater for larger events than isolated events (see figure 2), though they suffer from slightly worse spectral resolution due to additional read-noise and sub-threshold loss effects (figure 3). In photodiode and window timing mode, events are translated during the readout process resulting in the requirement for different event grading schemes and response files in these modes.[2] For all three modes, event grading is performed by the ground processing software. Because the various grade selections have different advantages, RMFs are made available for a number of event grade selection criteria in each mode.

Additionally, when Swift initially slews onto a new GRB, quick-look XRT spectra will be broadcast via the TDRSS satellite relay network and subsequently through the GCN. These spectra will be accumulated in photodiode and/or window timing mode but have no event recognition performed — i.e. they are ungraded. We have released non-event recognition RMFs for these modes.

Figure 2 shows the quantum efficiency curves for the standard grade selections of the various modes, while figure 3 provides a spectral response summary.

[2] A discussion of the effects of event translation in photodiode and window timing mode can be found in Mukerjee et al. (2003), while the grading scheme for all modes is described in Burrows et al. (in prep).

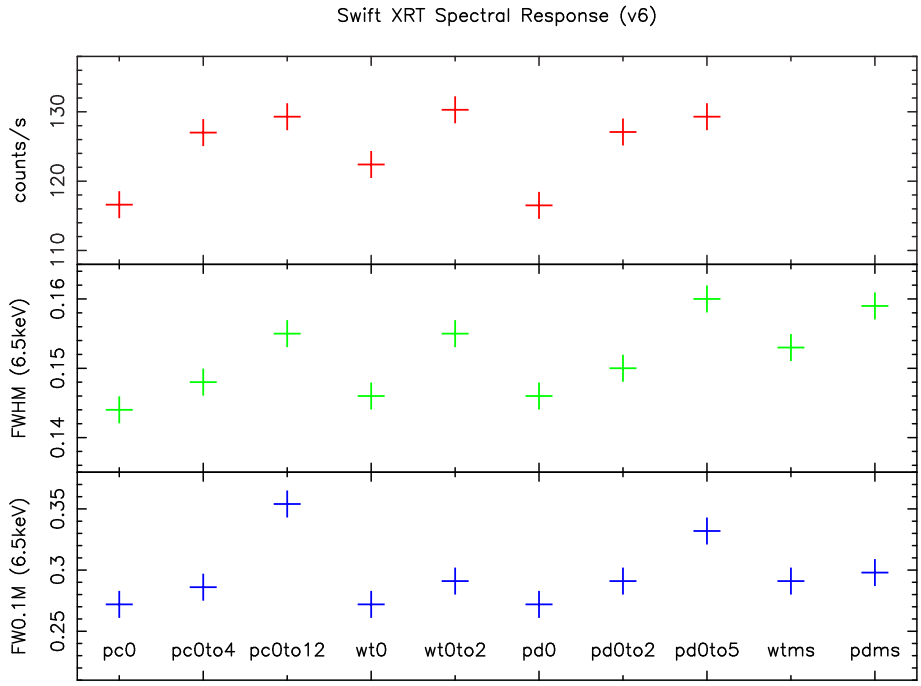

Figure 3: XRT spectral response summary for the various modes and grade selections for which RMFs have been made. The top panel shows the predicted $0.2 - 10.0$ keV count rate of an on-axis source with a power law spectrum of photon index 2.0, absorbed by a column of 10^{21} cm^{-2}. The source has a band-limited unabsorbed flux of 6.3×10^{-9} ergs cm^{-2} s^{-1}. The middle panel shows the full width at half maximum (in keV) of the response kernel at 6.5 keV, while the bottom panel shows the width at 10% of maximum.

4 Improvements made for this release

(i) Previously, loss functions, which are used by the simulator to describe how charge is lost near the surface of the device and manifests itself as a low energy tail to the response at low energies, were estimated from full frame calibration data obtained at Leicester. However, at the lowest energies (C at 0.277 keV; N at 0.392 keV), the effect has been shown to be non-uniform (see figure 4). New loss functions have therefore been generated for the central 200×200 region of the detector in order to better represent on-axis XRT pointings.

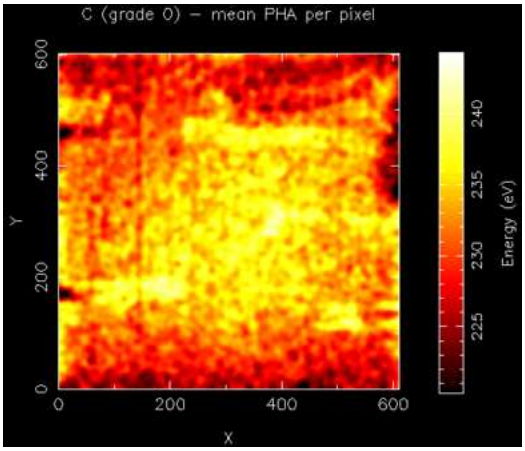

Figure 4: The spatial non-uniformity in the XRT spectral response is illustrated by the average event energy for C-K illumination (0.277 keV) over the face of the detector.

(ii) The magnitude of the Si-Kα line, produced by fluorescence within the detector, and its associated escape peak, has been refined to match the calibration data.

(iii) Modifications to the charge cloud spreading and associated charge loss fractions have been made for X-rays interacting in the field-free region of the detector with the aim of improving the line shoulder response at higher energies. However, see section 7 below.

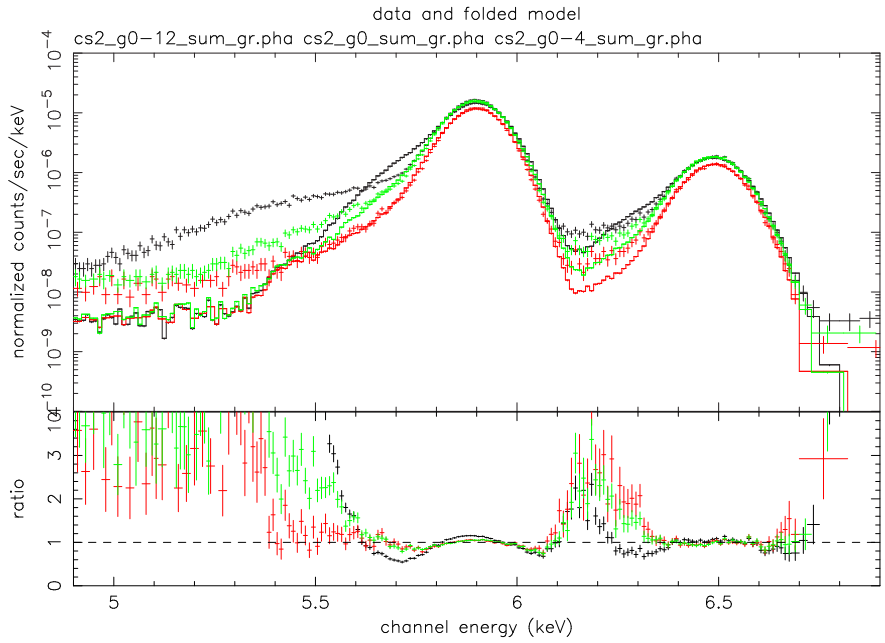

Figure 5: Mn-Kα (5.895 keV) and Mn-Kβ (6.490 keV) internal calibration source spectrum in photon counting mode. Key: black — grade 0–12; green — grade 0–4; red — grade 0. Crosses represent the data and histograms the model, consisting of two, narrow, gaussian lines.

(iv) The window timing response now correctly accounts for vertical event splitting at the row boundaries where the 10-row summations are performed.

(v) Non-event recognition RMFs have been generated for photodiode and window timing mode.

5 A comment on non-event recognition spectra

People with prior experience of astronomical X-ray CCD analysis will be familiar with the practise of event grading and selection of certain event grades to maximise the scientific return on the data — for example, isolated (or grade 0) events generally provide the best spectral resolution. The Swift XRT is unique in that non-event recognition spectra will be transmitted as soon as it slews onto a new GRB. Example non-event recognition spectra from calibration data can be seen in figures 6 & 7. These spectra reveal a prominent low energy tail to the redistribution kernel. The CCD response is naturally poorer under these circumstances and causes spectral features to become less significant compared to the times that event grading is available. For example, the apparent depth of the Al-K edge at 1.56 keV is reduced in figure 6(b) in the non-event recognition spectrum as redistribution from higher energies has filled in the feature.

6 Comparison with calibration data

Figures 5, 6 and 7 show X-ray spectral fits made to various calibration datasets using the released RMFs.

(i) Figure 5 shows the data and model for photon counting mode spectra obtained from the on-board Fe-55 corner calibration source which is located near the output anode (and suffers from minimal CTI effects) with three different grade selections: grade 0 (single pixel events, red), 0–4 (1 to 2 pixel events, green), and 0–12 (1 to 4 pixel events, black).

This shows that at higher energies the photon counting spectra are most accurately modelled for grade 0 events (down to 0.5% of the peak line intensity on the low energy side of the line), followed by grade 0–4 events (2%), with grade 0–12 poorest (18%) (though see section 7(ii)).

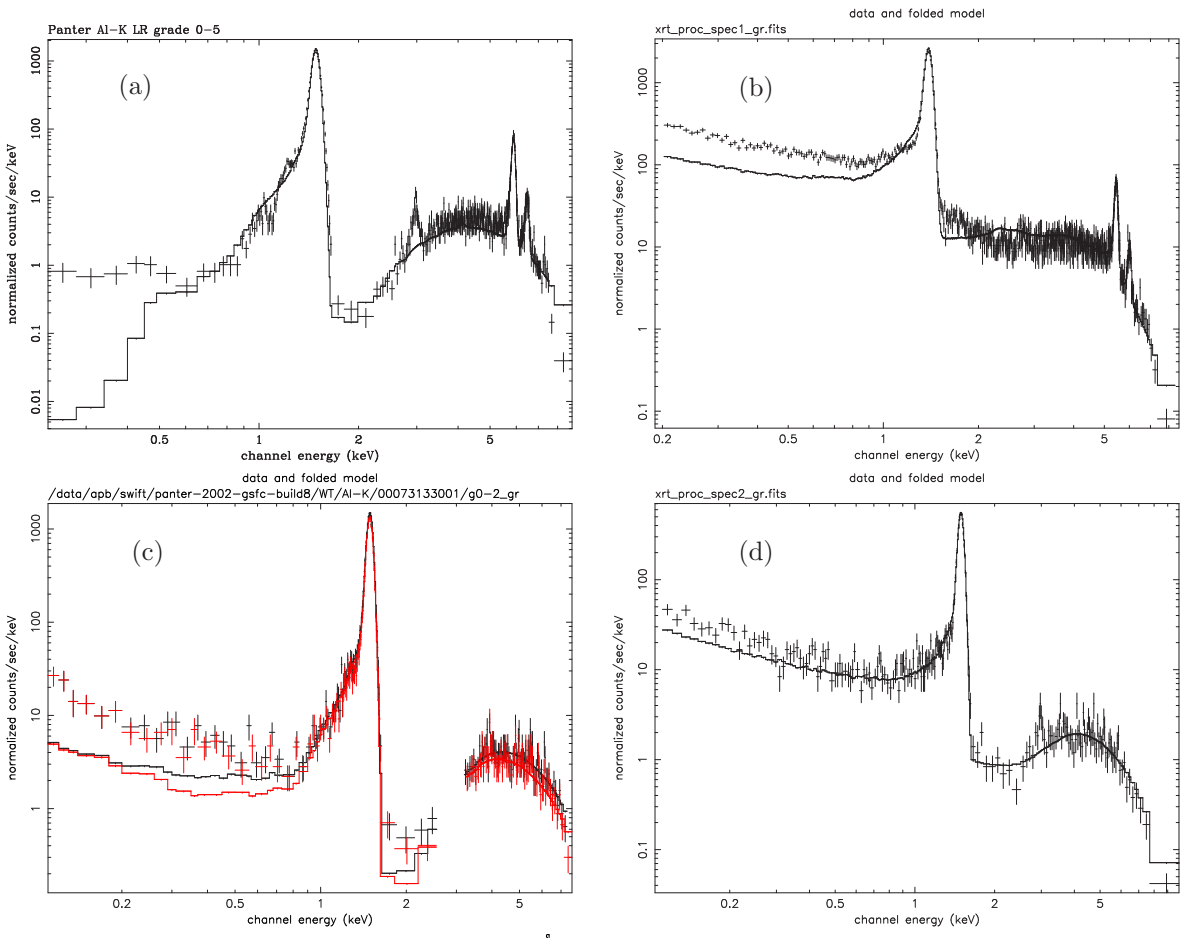

Figure 6: Al-K calibration data taken at the Panter X-ray Calibration Facility in Munich. (a) low rate photodiode mode (grade 0–5); (b) non-event recognition low rate photodiode mode; (c) window timing mode (black grade 0–2, red grade 0); (d) non-event recognition window timing mode. In all cases the model consists of a 6 keV bremsstrahlung continuum plus a narrow Al-K line at 1.487 keV, modified by a 10 micron thick aluminium absorption filter. Additional, narrow gaussians have been added at 5.895 keV and 6.490 keV to the photodiode mode models to account for the Mn-Kα,β corner source lines.

(ii) Figure 6 shows a selection of Al-K data taken at the Panter X-ray Calibration Facility in Munich, in both low rate photodiode and window timing modes, with and without event grading.

At this energy the graded spectra are dominated by single pixel events and are accurately modelled to about 0.3% of the peak line intensity.

(iii) Figure 7 shows Fe-K data, also taken at Panter, in window timing mode, with and without event grading.

At this energy the graded spectra are modelled to about 6% of the peak line energy for both window timing grade selections.

We emphasise these fit comparisons are based on high quality ground calibration data and the discrepencies between this data and the response model are often well below the level that will be reached statistically in orbit. Spectral fits to observations are expected to show residuals less than 5%, presuming no change in the response.

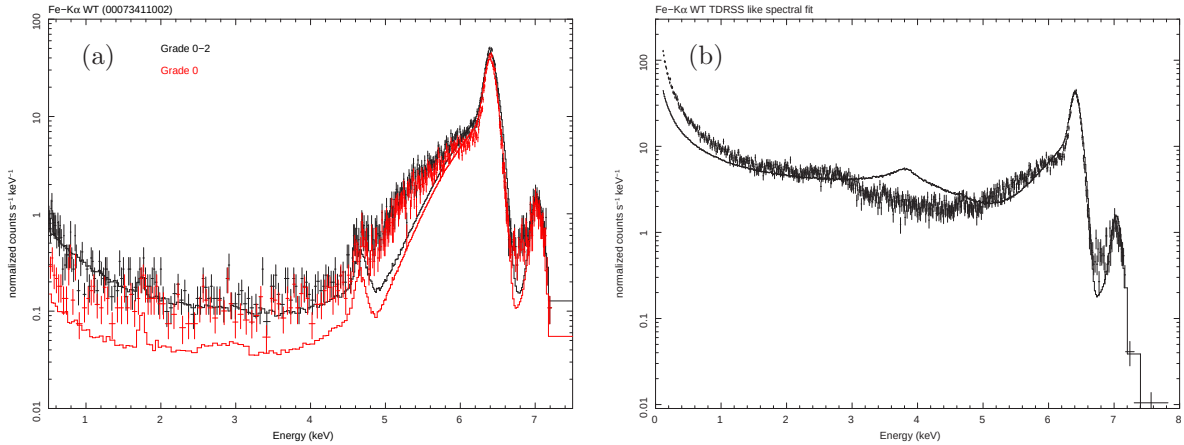

Figure 7: Fe-K calibration data from Panter. (a) window timing mode (black grade 0–2, red grade 0); (b) non-event recognition window timing mode. In both cases the model consists of a 5 keV bremsstrahlung continuum plus narrow Fe-Kα, β lines at 6.4 keV and 7.06 keV, modified by a 50 micron thick iron absorption filter.

7 Limitations of the released RMFs

(i) While we have endeavoured to make the most accurate response for the central regions of the CCD, it is clear from figure 4 that there is a spatial gain effect at low energies towards the outer regions of the detector. Spectral analysis should be performed with caution below 0.4 keV on sources which appear outside the central 200×200 region of the CCD.

(ii) The large event size response does not accurately model the low energy wing of high energy lines. This is most obvious in the Mn-Kα photon counting spectra shown in figure 5 and to a lesser extent in the window timing Fe-Kα spectra in figure 7. The origin of the discrepancy is under investigation, but is thought to be related to the effects of sub-threshold losses on event reconstruction.

To quantify this further, we created a test photon counting mode RMF where the event threshold was set artificially high. This enables the low energy wing of the 5.895 keV line to be modelled more accurately for grade 0–12 events. Using this test RMF we faked a simple absorbed power-law spectrum (with a column density of $10^{21}\mathrm{cm}^{-2}$, and a photon index of 2), then fit it with the v6 RMF. We found the spectral parameters were recovered to within 2%, though the fit residuals showed an apparent edge at the 5% level near 1.5 keV, just below the Si-K region.

When using the large event RMFs users should be wary of apparent spectral features near this energy.

(iii) The 'loss-shelf', which is apparent as a low energy (< 0.5 keV) continuum in the low rate photodiode mode spectrum of Al-K in figure 6(a), is currently not modelled accurately in the RMFs. This would be seen as excess emission at low energies for heavily absorbed sources at the $0.1 - 0.5\%$ peak flux level.

(iv) While not strictly an RMF related issue, we re-emphasise that photodiode mode contains events from the entire CCD. This includes the Fe-55 calibration sources (i.e. Mn-Kα at 5.895 keV and Mn-Kβ at 6.490 keV), located at the corners of the detector. Because this is a background, rather than a response effect, the photodiode mode RMFs do not specifically take into account this emission.

(v) The RMF generator does not account for pile-up and can only be reliably used on data that is free from pile-up.

(vi) The photodiode mode RMFs should be used with caution when modelling Panter calibration data taken in this mode (for example, for training purposes), especially if the data are in non-event recognition form. The photodiode mode gain was different during the Panter calibration campaign (2.73 eV/chan) and has since been brought into line with the other modes (2.53 eV/chan). The

RMFs were generated assuming the latter value. However, this can be compensated for by careful use of the 'gain fit' command in XSPEC.

8 Future developments

We continue to develop the XRT CCD response model. Future RMF releases may include:

- Improvements to the large event size response at high energies will follow once the sub-threshold loss effects are better understood and modelled.
- A new model for the loss-shelf will be investigated.
- Off-axis RMFs with a more accurate response below 0.4 keV.
- Response model parameters tuned to reflect in-orbit performance.

9 The RMFs released this time

swxpc0_20010101v006.rmf	PC mode grade 0
swxpc0to4_20010101v006.rmf	PC mode grade 0–4
swxpc0to12_20010101v006.rmf	PC mode grade 0–12
swxpd0_20010101v006.rmf	PD mode grade 0
swxpd0to2_20010101v006.rmf	PD mode grade 0–2
swxpd0to5_20010101v006.rmf	PD mode grade 0–5
swxwt0_20010101v006.rmf	WT mode grade 0
swxwt0to2_20010101v006.rmf	WT mode grade 0–2
swxpdmspha_20010101v006.rmf	PD mode non-event recognition (TDRSS)
swxwtmspha_20010101v006.rmf	WT mode non-event recognition (TDRSS)

REFERENCES

D.N. Burrows et al. The Swift X-ray Telescope. *Space Science Reviews*, in prep.

K. Mukerjee, A.F. Abbey, and J. Osborne. Selection of the Swift XRT event pattern library and event pattern relationships. Technical Report LUX-TN-100, Leicester University, 2003.

K. Mukerjee et al. The Spectroscopic performance of the Swift X-ray Telescope for Gamma-Ray Burst studies. *Proc. SPIE*, 5165:251–261, 2004.